

# Phase transformations of eutectoid Zn-Al alloys

YAO HUA ZHU

*Instituto de Investigaciones en Materiales, UNAM, Mexico**E-mail: yaohua@servidor.unam.mx*

Systematic investigations on microstructures and phase transformations were carried out on solution treated, chilled as-cast and extruded Zn-Al based alloys (containing small amounts of Cu or Cu and Si). Phase transformation sequences of the thermal and thermomechanically treated eutectoid Zn-Al alloys were studied along with isothermal holding. Two new unstable phases  $\eta'_S$  and  $\eta'_E$  and their decomposition products in the chilled as-cast and extruded eutectoid Zn-Al alloys are discussed.

© 2001 Kluwer Academic Publishers

## 1. Introduction

Superplasticity has been known to occur in Zn-22%Al based eutectoid alloys since 1945 [1–4]. An overall understanding of the superplasticity of these alloys along with microstructural development and phase transformations have been of interest from in both on industrial and an academic perspective. The phase diagrams of both the ternary Zn-Al-Cu alloy system and quaternary Zn-Al-Cu-Si alloy system have been determined. A series of equilibrium solid state phase transformations below 350°C have been established as follows,

$$\beta + T' = \alpha + \varepsilon \quad \text{at } 285^\circ\text{C}$$

$$\beta + \varepsilon = \alpha + \eta \quad \text{at } 276^\circ\text{C}$$

$$\alpha + \varepsilon = T' + \eta \quad \text{at } 268^\circ\text{C}$$

where  $\beta$  is Zn rich f.c.c. phase,  $\alpha$  is Al rich f.c.c. phase,  $\varepsilon$  is h.c.p. phase  $\text{CuZn}_4$  and  $\eta$  is Zn rich h.c.p. phase [5–7].  $T'$  is a rhombohedral structure phase Zn<sub>10</sub>Al<sub>35</sub>Cu<sub>55</sub> (in wt%). Little systematic investigation has been done on ageing characteristics, structural developments and effects of alloying on the superplasticity of the eutectoid Zn-Al based alloys (containing small amounts of Cu or Cu and Si). The purpose of the present paper is to establish a systematic understanding of the microstructures and phase transformations of the eutectoid Zn-Al based alloys being treated under different thermal and thermomechanical treatments, i.e. solution treated, chilled as-cast and extruded conditions, based on the well established equilibrium phase relationships of the alloy systems.

## 2. Experimental

Two eutectoid Zn-Al based alloys Zn<sub>75</sub>Al<sub>20</sub>Cu<sub>3</sub>Si<sub>2</sub> and Zn<sub>76</sub>Al<sub>22</sub>Cu<sub>2</sub> (both in wt%) were prepared from 99.99% Zn, 99.99% Al, high purity Cu and Si, induction melted in a graphite crucible and cast at 700°C into a preheated mild steel mould. Specimens for solution treatment were cut from the 400°C rolled in-

got, then solution treated at 350°C for 2 days, followed by quenching in ice water and ageing at temperatures ranged 50–170°C.

The chilled as-cast specimen was made by water spray cooling of the solidified ingot after one minute air cooling, then cut into pieces for X-ray diffraction examination and observation both on optical and scanning microscopies during ageing at 90.4°C.

The eutectoid Zn-Al alloy Zn<sub>76</sub>Al<sub>22</sub>Cu<sub>2</sub> (in wt%) was continuously cast into rods, then extruded into rods after heating up to 250°C. The extruded specimens were aged at 150°C.

Special care was taken on X-ray diffraction examination at the early stage of ageing for both solution treated and chilled as-cast eutectoid specimens. Phase transformations were determined from the diffraction peak positions which were reported using nickel filtered Cu K $_{\alpha}$  radiation and a diffractometer scanning at a speed of 1 deg/min.

Conventional optical and scanning microscopy were applied for microstructural observations during isothermal holding. Compositions of various phases involved in the present investigation were determined by using Electron Probe Microanalysis.

## 3. Results and discussion

### 3.1. Microstructures of eutectoid Zn-Al based alloys

#### 3.1.1. Solution treated and chilled as-cast states

As shown in the X-ray diffractograms, Fig. 1, the 350°C solution treated eutectoid alloy consisted of three phases  $\beta'_S$ ,  $\varepsilon$  and  $\sigma$ . The  $\beta'_S$  phase is a supersaturated phase in the as-quenched eutectoid alloy Zn<sub>75</sub>Al<sub>20</sub>Cu<sub>3</sub>Si<sub>2</sub> (in wt%), where Si rich  $\sigma$  phase appeared as isolated particles. These have a minor effect on the phase transformations of Zn-Al based alloys [7, 8]. However typical dendritic structures were observed to possess the supersaturated phases  $\alpha'_S$ ,  $\beta'_S$ ,  $\eta'_S$  and  $\varepsilon$  in the chilled as-cast eutectoid alloy. The

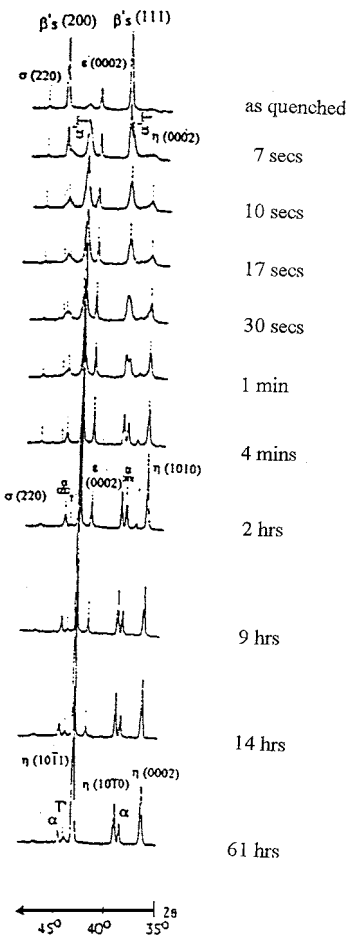


Figure 1 X-ray diffractograms of alloy AlZn75Cu3Si2 aged at 150°C.

diffraction peaks of  $\alpha'_S$  and  $\beta'_S$  phase appeared overlapped on the X-ray diffractograms, Fig. 2. The newly found Zn rich  $\eta'_S$  phase was determined to have an hexagonal close packed crystal structure in the chilled as-cast alloy. The X-ray diffraction peaks of overlapped  $\alpha'_S$  and  $\beta'_S$  phases appeared at  $2\theta = 45.5^\circ$  for crystal plane (200). The X-ray diffraction peaks from crystal planes (0002), (10 $\bar{1}$ 0) and (10 $\bar{1}$ 1) of the  $\eta'_S$  phase appeared at  $2\theta = 37.1^\circ$ ,  $2\theta = 39.1^\circ$  and  $2\theta = 43.3^\circ$ .

Metallographic observations using both optical and scanning microscopy showed that the supersaturated  $\beta'_S$  phase was the matrix of the structure and small particles of  $\epsilon$  phase appeared as second phase in the solution treated alloy, shown in Fig. 3, while more supersaturated phases  $\alpha'_S$ ,  $\beta'_S$ ,  $\eta'_S$  and  $\epsilon$  formed in the chilled as-cast eutectoid alloy due to the complex solidification process of the cast alloy, shown in Fig. 4. Al rich  $\alpha'_S$  phase solidified first from the melt as cores of dendrites. With continuous solidification, the composition of the  $\alpha'_S$  phase around the first solidified  $\alpha'_S$  phase gradually changed to the composition of  $\beta'_S$  phase. The  $\beta'_S$  phase appeared at the edges of the  $\alpha'_S$  phase, around the cores of the dendrites. Due to the continuous cooling, there was no apparent phase boundary observed in the cast eutectoid alloy. The average compositions of  $\alpha'_S$  and  $\beta'_S$  phases were determined and are shown in Table I.

The  $\eta'_S$  phase and  $\epsilon$  phase finally solidified to form the interdendritic regions, where  $\alpha$  phase particles were observed, as shown in Fig. 4a, meaning that the newly

TABLE I Average compositions of  $\alpha'_S$  and  $\beta'_S$  phases in chilled as cast eutectoid Zn-Al alloy

| wt %        | Zn   | Al   | Cu  |
|-------------|------|------|-----|
| $\alpha'_S$ | 64.9 | 33.3 | 1.8 |
| $\beta'_S$  | 75.6 | 21.8 | 2.6 |

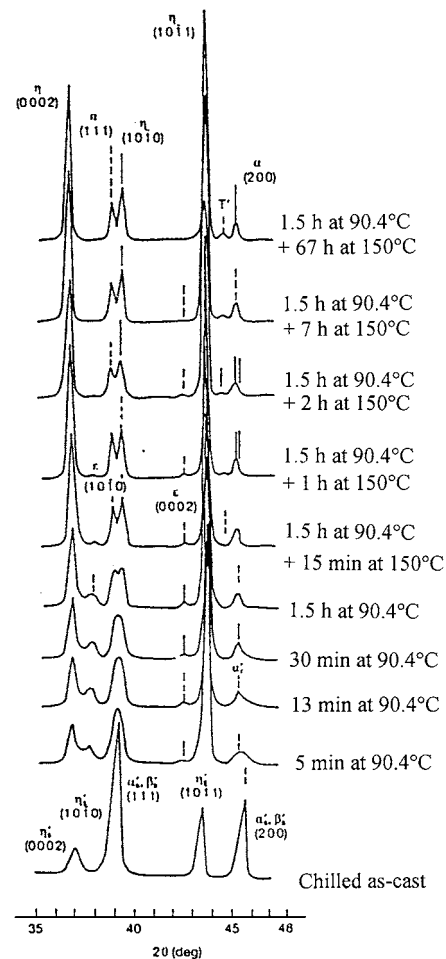


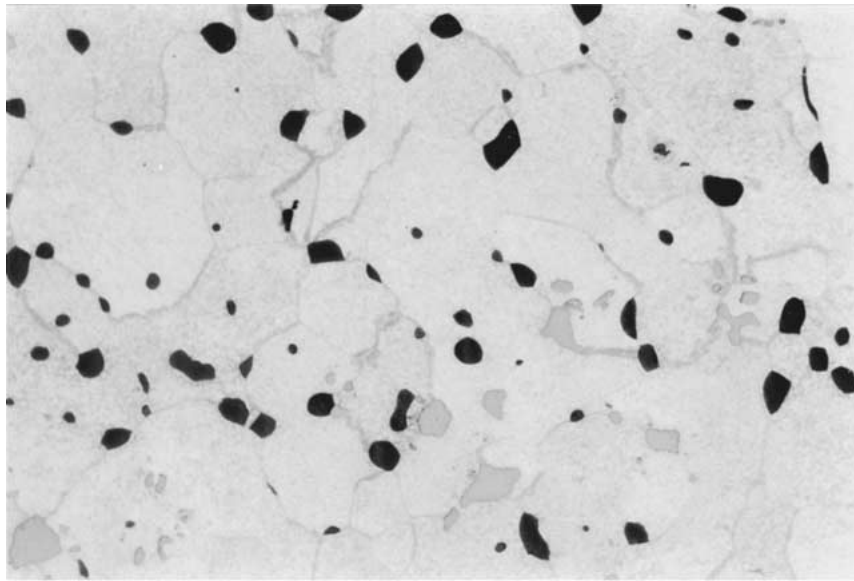
Figure 2 X-ray diffractograms of the chilled as cast eutectoid Zn-Al (ZnAl22Cu2) during ageing.

found  $\eta'_S$  phase was unstable, even at room temperature decomposed during specimen preparation and observation, as the  $\eta$  phase did not appear initially from the X-ray diffractogram of the chilled as cast alloy, shown in Fig. 2.

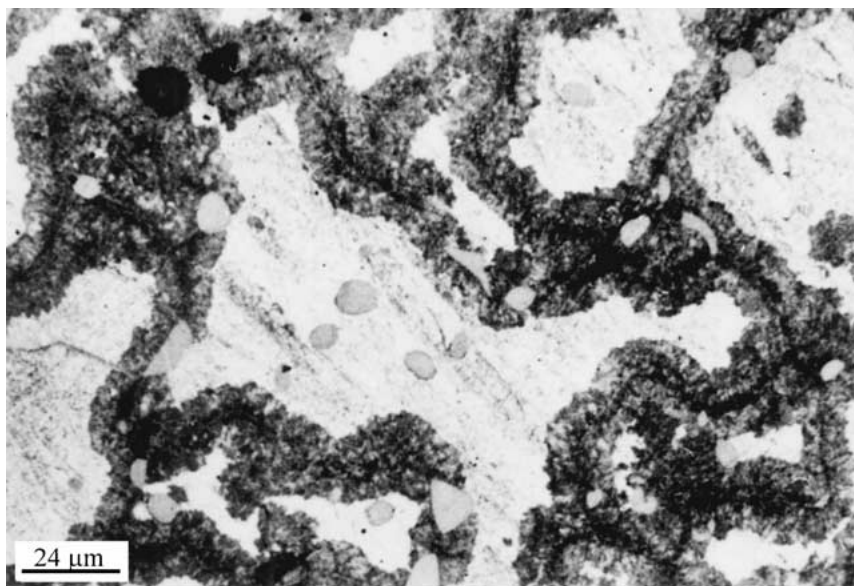
### 3.1.2. Extruded state

With the extruded eutectoid Zn-Al alloy, the X-ray diffraction results showed in Fig. 5 that there were three phases  $\alpha$ ,  $T'$  and  $\eta'_E$  existing after 250°C extrusion. the  $\eta'_E$  phase was a newly found phase of zinc rich hexagonal close packed structure. The diffraction peaks of  $\alpha$  phase appeared at  $2\theta = 38.7^\circ$  for crystal plane (111) and  $2\theta = 44.9^\circ$  for crystal plane (200). The diffraction peaks from crystal planes (0002), (10 $\bar{1}$ 0) and (10 $\bar{1}$ 1) of  $\eta'_E$  phase appeared at  $2\theta = 36.9^\circ$ ,  $39.1^\circ$  and  $43.3^\circ$ .

During extrusion at 250°C, the continuous cast eutectoid alloy underwent thermomechanical treatments.



a



b

Figure 3 Optical micrograph of alloy AlZn75Cu3Si2 (a) as-quenched (b) after 0.5 min ageing at 100°C.

Both the  $\alpha'_S$  and  $\beta'_S$  phases decomposed into  $\alpha_f$  phase, i.e.  $\alpha$  phase in the extruded alloy. The X-ray diffraction peaks of both  $\alpha'_S$  and  $\beta'_S$  phases disappeared from the X-ray diffractograms at  $2\theta = 45.5^\circ$  for crystal plane (200), as shown in Fig. 2. Instead, the diffraction peaks of  $\alpha$  phase appeared at  $2\theta = 38.7^\circ$  for crystal plane (111) and  $2\theta = 44.9^\circ$  for crystal plane (200), as shown in Figs 2 and 5. The supersaturated  $\eta'_S$  phase decomposed and transformed into the  $\eta'_E$  phase after 250°C extrusion. The  $\eta'_E$  phase appeared at different  $2\theta$  positions, compared with  $\eta'_S$  phase of chilled as cast eutectoid alloy. The composition of the eutectoid Zn-Al alloy is located within three phase field ( $\alpha$ ,  $\eta$  and  $T'$ ) below 268°C [5–7] therefore the  $\varepsilon$  phase deduced from decomposed  $\alpha'_S$  phase and  $\beta'_S$  phase disappeared under 250°C extrusion in the four phase transformation,  $\alpha + \varepsilon \rightarrow T' + \eta$  (discussed in the following section).

Scanning electron micrographs of the extruded eutectoid Zn-Al alloy are shown in Fig. 6. The microstructure of the extruded alloy consisted of the decomposed  $\alpha'_S$  phase, appearing as dark isolated particles with clear phase boundaries and the bright  $\eta'_E$  phase dispersed in the decomposed  $\beta'_S$  phase region. In the chilled as-cast alloy, the  $\beta'_S$  phase appeared as an edge of the dendrite core  $\alpha'_S$  phase. After 250°C extrusion, the  $\beta'_S$  phase decomposed and the X-ray diffraction peaks of the  $\beta'_S$  phase disappeared from the diffractograms.

The lattice parameters of  $\varepsilon$ ,  $\eta$  and the newly found  $\eta'_S$  and  $\eta'_E$  phases were respectively determined and listed for comparison in Table II.

It was interested to find that the lattice parameters  $c_0/a_0$  ratio of the supersaturated zinc rich phases  $\eta'_S$  and  $\eta'_E$  were smaller than the final stable  $\eta$  phase because of different thermal and thermo-mechanical treatments.

TABLE II Lattice parameters of  $\epsilon$ ,  $\eta'_S$ ,  $\eta'_E$  and  $\eta$  phases

|            | $a_0$ (nm) | $c_0$ (nm) | $c_0/a_0$ |
|------------|------------|------------|-----------|
| $\epsilon$ | 0.2767     | 0.4289     | 1.550     |
| $\eta'_S$  | 0.2668     | 0.4842     | 1.815     |
| $\eta'_E$  | 0.2663     | 0.4872     | 1.829     |
| $\eta$     | 0.2671     | 0.4946     | 1.852     |

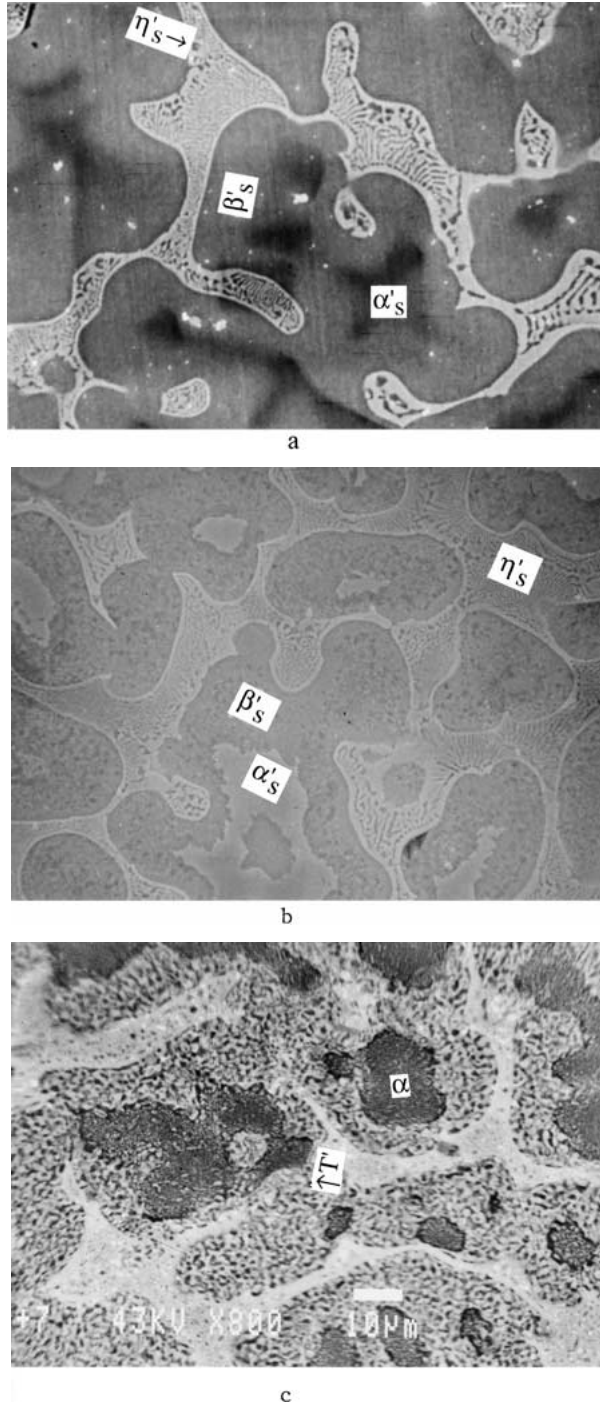


Figure 4 Scanning electron micrographs of as cast eutectoid Zn-Al alloy, (a) chilled as cast state, (b) after 30 seconds ageing at 90.4°C, (c) after 1.5 hours ageing at 90.4°C and 67 hrs at 150°C.

This induced various supersaturated phases of different chemical compositions, in other words, dissolving Al and Cu in Zn rich phase changed the dimension of the unit cell of the crystal structure. This might affect phys-

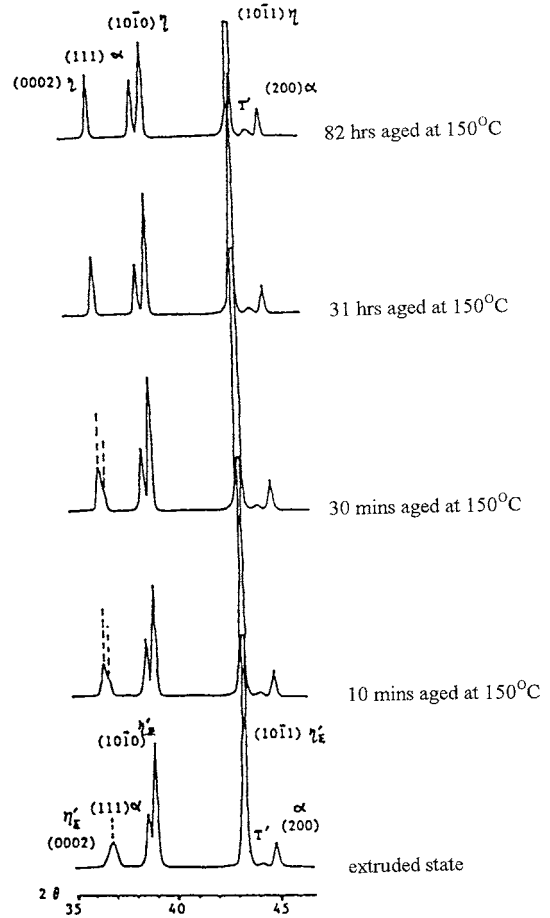


Figure 5 X-ray diffractogram of extruded eutectoid Zn-Al alloy during ageing at 150°C.

ical and mechanical properties, especially dimensional stability of the alloy.

### 3.2. Phase transformations during isothermal holding

The supersaturated phases of both solution treated and chilled as-cast eutectoid alloys were unstable and rapidly decomposed during isothermal holdings. The determinations of X-ray diffraction in the early stage of ageing were carried out with great care. The X-ray diffraction results are shown in Figs 1 and 2.

The  $\beta'_S$  phase of solution treated alloys decomposed within 10 seconds of ageing at 150°C, as a cellular reaction,  $\beta'_S \rightarrow \alpha'_T + \epsilon + \eta$ . The diffraction peaks of  $\beta'_S$  phase decreased in height, meanwhile the diffraction peaks of  $\alpha'_T$ ,  $\epsilon$  and  $\eta$  phases increased in height, shown in Fig. 1. Fig. 3b showed that the decomposition of  $\beta'_S$  phase occurred at the grain boundaries as discontinuous precipitation. The lattice parameter of  $\alpha'_T$  phase was 0.4051 nm, very close to the lattice parameter, 0.4048 nm, of the equilibrium  $\alpha$  phase at 275°C. That meant the decomposition of  $\beta'_S$  phase, i.e.  $\beta'_S \rightarrow \alpha'_T + \epsilon + \eta$ , was correlated with the equilibrium reaction  $\beta + \epsilon = \alpha + \eta$  at 276°C. With eutectoid alloy composition,  $\beta$  phase disappears just below the equilibrium reaction temperature 276°C according to the phase diagrams [5, 6].

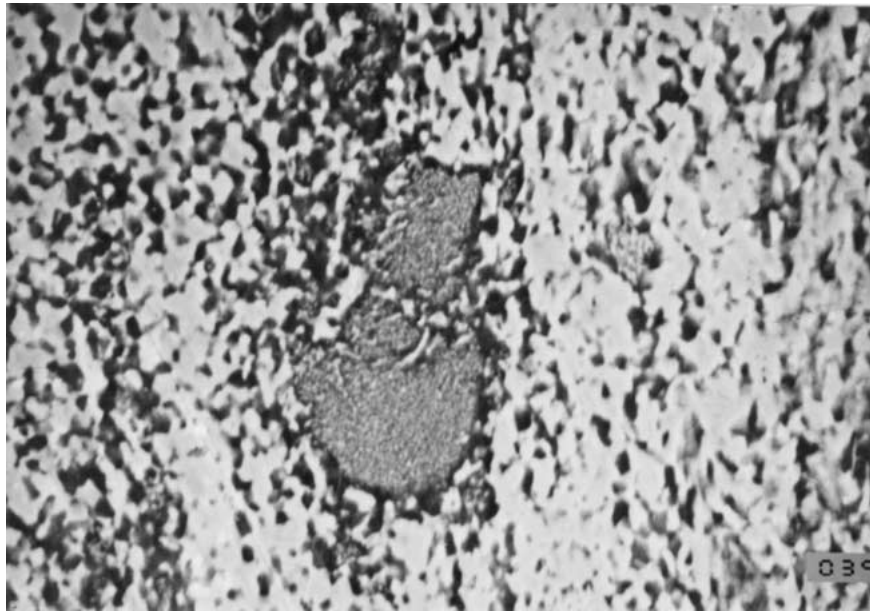


Figure 6 Scanning electron micrographs of extruded eutectoid alloy, as extruded state X 1500.

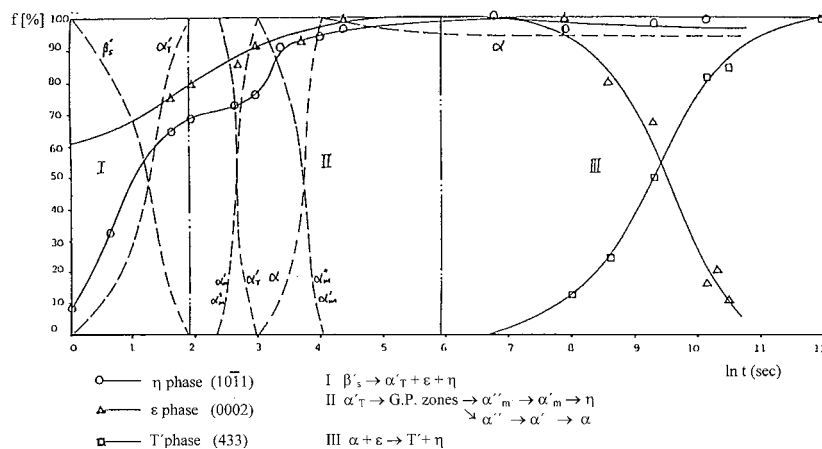


Figure 7 Fractional transformation curves of phases in alloy AlZn75Cu3Si2 aged at 170°C.

It was found that about 70% of  $\varepsilon$  and  $\eta$  phases formed in the early stage of ageing, indicating that the decomposition of  $\beta'_S$  phase was the most important incoherent precipitation during ageing, as shown in Fig. 7.

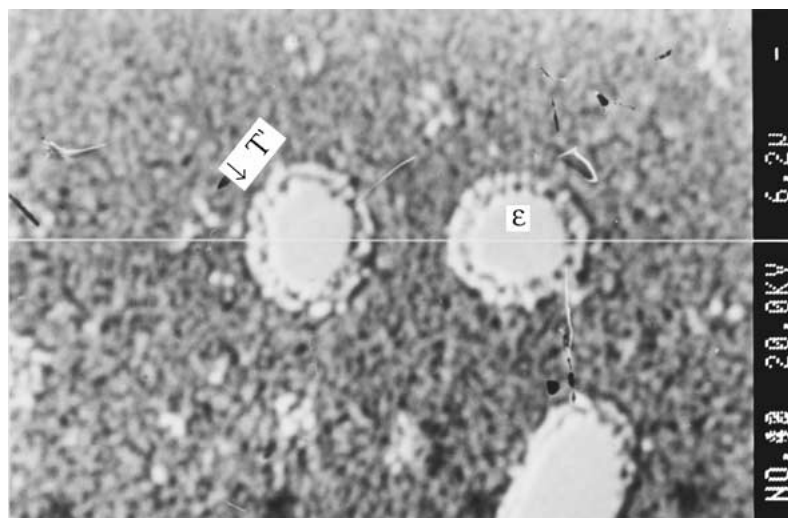
In the subsequent ageing, the X-ray diffraction peaks of  $\alpha'_T$  phase shifted gradually to the lower  $2\theta$  angles. The continuous precipitation lead the composition modulation of the metastable phase  $\alpha'_T$  towards to  $\alpha$  phase by formation of zinc rich transition phases of  $\alpha''_m$  and  $\alpha'_m$ , and Al rich  $\alpha''$  and  $\alpha'$  transitional phases in equilibrium with  $\alpha''_m$  and  $\alpha'_m$ , i.e. the spinodal decomposition occurred [6, 8]. The fractional transformation of both  $\varepsilon$  and  $\eta$  increased gradually to the maximum as shown in Fig. 7.

During prolonged ageing, a four phase transformation:  $\alpha + \varepsilon \rightarrow T' + \eta$ , occurred. The diffraction peaks of  $\varepsilon$  phase decreased in height and finally vanished and left diffraction peaks of  $T'$  phase that were stable on the X-ray diffractograms, as shown in Fig. 1. The fractional transformation curves of phases showed as well the four phase transformation in Fig. 7. The

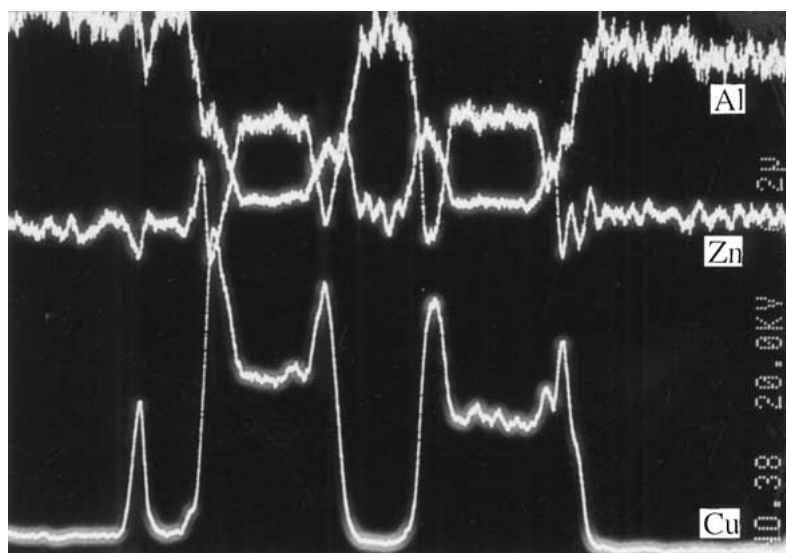
SEM X-ray line scanning showed in Fig. 8 that  $T'$  phase particles formed at the  $\varepsilon$  phase boundaries, where fairly strong Al and Cu X-ray intensities and weaker Zn X-ray intensity were observed in accordance with the chemical composition of  $T'$  phase (10%Zn-35%Al-55%Cu).

The decomposition of  $\beta'_S$  phase of chilled as-cast alloy was detected in the early stage of ageing, as shown in Fig. 2. After 30 seconds ageing at 90.4°C, the  $\beta'_S$  phase around the  $\alpha'_S$  phase apparently decomposed similar with the discontinuous precipitation of the  $\beta'_S$  phase in the solution treated alloy,  $\beta'_S \rightarrow \alpha'_T + \varepsilon + \eta$ , shown in Fig. 4b.

It was detected from X-ray diffraction examinations that both  $\alpha'_S$  and  $\beta'_S$  phases decomposed into  $\alpha'_T$ ,  $\varepsilon$  and  $\eta$  phases after 5 minutes ageing at 90.4°C. Both peaks of  $\alpha'_S$  and  $\beta'_S$  phases decreased in their heights, while three sets of peaks of  $\alpha'_T$ ,  $\varepsilon$  and  $\eta$  phases grew up. The decomposition completed after about 30 minutes ageing at 90.4°C, both  $\alpha'_S$  and  $\beta'_S$  phases disappeared on the X-ray diffractograms, as shown in Fig. 2.



a



b

Figure 8 Scanning electron micrograph of alloy AlZn75Cu3Si2 aged at 100°C for 6 h, (b) SEM X-ray scanning line showing the Zn, Al and Cu distribution in the alloy microstructure shown in Fig. 8(a).

During prolonged ageing, the phase transformations, i.e. the spinodal decomposition and the four phase transformation, were found to be similar to the solution treated alloy. The  $\alpha'_T$  and  $\alpha'_S$  shifted to the lower  $2\theta$  angles on the X-ray diffractograms and  $\alpha$  formed. After 1.5 hours ageing at 90.4°C the diffraction peaks of  $\varepsilon$  phase vanished and the diffraction peak of  $T'$  phase occurred at 44.3°. SEM observation showed that the  $T'$  phase formed both in the interdendritic regions and in the decomposed  $\beta'_S$  boundaries in Fig. 4c.

In the extruded alloy, the newly determined  $\eta'_E$  phase was found to decompose during the isothermal holding. It was identified characteristically that the X-ray diffraction peak of crystal plane (0002) of  $\eta'_E$  phase at  $2\theta = 36.9^\circ$  decreased gradually in height in the early stage of ageing, accompanying the appearance and increase in height of the diffraction peak of crystal plane (0002) of  $\eta$  phase at  $2\theta = 36.3^\circ$ . Meanwhile, the diffrac-

tion peaks of  $T'$  and  $\eta$  phases increased in height. The diffraction peak of  $\eta'_E$  phase at  $2\theta = 36.9^\circ$  disappeared after about 1 hour ageing at 150°C, as shown in Fig. 5. The relative X-ray diffraction intensities of phases  $T'$  (433) and  $\alpha$  (200) at 91° and 150°C were measured and plotted in Fig. 9. It was obvious to conclude that the  $\eta'_E$  phase decomposed into three phases ( $\alpha$ ,  $\eta$  and  $T'$ ), i.e.  $\eta'_E \rightarrow \eta + \alpha + T'$ .

It was also found that the diffraction peaks of the three phases ( $\alpha$ ,  $\eta$  and  $T'$ ) were at the same  $2\theta$  angle positions compared with equilibrium phases ( $\alpha + \eta + T'$ ) at 268°C. That implied that the decomposition of the  $\eta'_E$  phase was correlated with the equilibrium,  $\alpha + \varepsilon = T' + \eta$ , at 268°C. After the decomposition of the  $\eta'_E$  phase, the extruded alloy was consisted of three stable phases ( $\alpha$ ,  $\eta$  and  $T'$ ), which were same as the stable phases both in solution treated and chilled as-cast eutectoid Zn-Al alloy, as shown in Fig. 10.

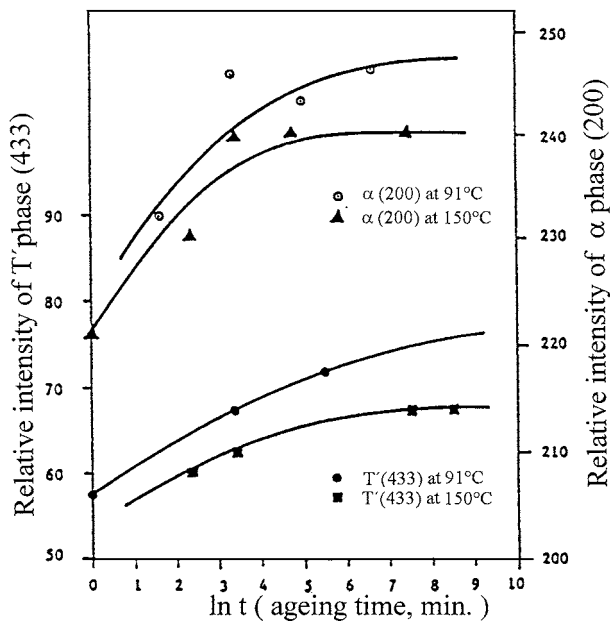


Figure 9 Relative X-ray diffraction intensities of  $\alpha(200)$  and  $T'(433)$  at 91°C and 150°C.

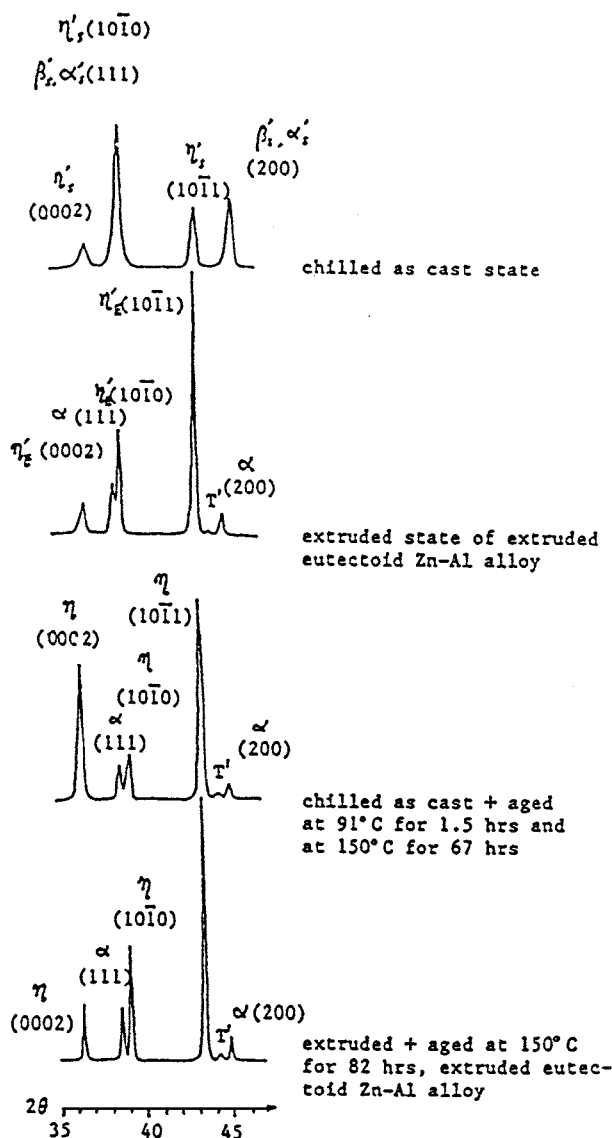
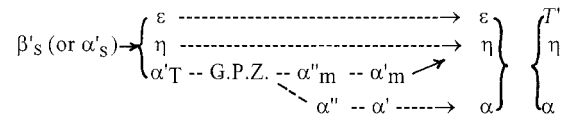


Figure 10 Comparison of X-ray diffractograms of various states of eutectoid Zn-Al alloy.

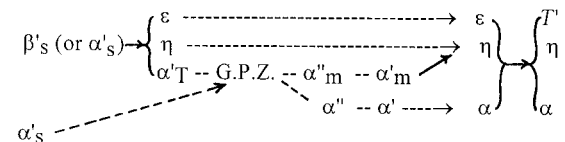
#### 4. Conclusions

1. The microstructure of 350°C solution treated eutectoid Zn-Al based alloy (containing small amount of Cu/Cu and Si) consisted basically of supersaturated  $\beta'_S$  and  $\epsilon$  phases. The phase transformation sequences of the supersaturated  $\beta'_S$  phase during isothermal holding were as follows,



2. The microstructure of chilled as cast eutectoid Zn-Al based alloy (containing small amount of Cu or Cu and Si) consisted of supersaturated  $\alpha'_S$ ,  $\beta'_S$ ,  $\eta'_S$  and  $\epsilon$  phases, appeared as a typical dendritic structure. The  $\alpha'_S$  phase was the core surrounded by the supersaturated  $\beta'_S$  phase. The newly found  $\eta'_S$  phase and  $\epsilon$  phase solidified finally to form the interdendritic region.

The phase transformation sequences during isothermal holding were as follows,



3. The microstructure of the 250°C extruded eutectoid Zn-Al based alloy consisted of three phases  $\alpha$ ,  $T'$  and  $\eta'_E$ . The newly found  $\eta'_E$  phase dispersed in the decomposed  $\beta'_S$  phase region. During isothermal holding, the  $\eta'_E$  phase decomposed into three phases ( $\alpha$ ,  $\eta$  and  $T'$ ), i.e.  $\eta'_E \rightarrow \eta + \alpha + T'$ .

4. The decompositions of  $\beta'_S$  phases in the solution treated eutectoid alloy and in the chilled as-cast eutectoid alloy, i.e.  $\beta'_S \rightarrow \alpha'_T + \epsilon + \eta$  and  $\beta'_S$  (and  $\alpha'_S$ )  $\rightarrow \alpha'_T + \epsilon + \eta$ , were correlated to the 276°C equilibrium reaction:  $\alpha + \epsilon = T' + \eta$ .

The four phase transformations,  $\alpha + \epsilon \rightarrow T' + \eta$ , occurred during the prolonged ageing both in solution treated and the chilled as cast eutectoid Zn-Al based alloy, which were correlated to the 268°C equilibrium reaction:  $\alpha + \epsilon = T' + \eta$ .

The decomposition of the  $\eta'_E$  phase in the extruded eutectoid Zn-Al based alloy was correlated to the 268°C equilibrium reaction:  $\alpha + \epsilon = T' + \eta$ .

5. The final stable phases of the prolonged aged eutectoid Zn-Al alloy of same chemical composition were the same  $\alpha$ ,  $\eta$  and  $T'$  phases no matter what kind of thermal and thermo-mechanical treatments were initially taken.

6. The  $c_0/a_0$  ratios of the cph phases  $\eta'_S$ ,  $\eta'_E$  and  $\eta$  phases were determined as the following series,

$$\eta'_S(1.815) < \eta'_E(1.829) < \eta(1.852).$$

Various thermal and thermo-mechanical treatments induced supersaturated phases of different lattice parameters. Dissolving Al and Cu in zinc rich  $\eta$  phase changed the dimensions of the unit cell of the crystal structure which might affect physical and mechanical

properties, especially the dimensional stability of the alloy.

### Acknowledgements

The author thanks P. Det, Leticia Baños, Jose Guman and Antonio Caballero for their help in the experimental work.

### References

1. A. A. BOCHER and Z. A. SVIDRSKAIA, *Izv Akad Nauk SSSR Otde Tekh Nauk* **9** (1945) 821.
2. E. E. UNDERWOOD, *Journal of Metals* **14** (1962) 91.

3. W. A. BACKOFEN, I. R. TURNER and D. H. AVERY, *AMS Transactions* **57**(4) (Dec. 1964).
4. A. BALL and M. M. HUTCHINSON, *Metals Science Journal* (1969).
5. S. MURPHY, *Journal of Metal Science* **9** (1975) 163.
6. Y. H. ZHU, Ph.D. thesis, University of Aston, UK, 1983.
7. *Idem.*, *Chin. J. Met. Sci. Techn.* **5** (1989) 113.
8. Y. H. ZHU, T. SANVANSKAN and S. MURPHY, *Mat. Res. Soc. Proc.* **21** (1984) 835.

*Received 8 February 2000  
and accepted 28 March 2001*